Reliability of HSS Cross Connections in Branch Axial Compression

Dillon F. Rudman, Quanhan Xi, Jeffrey A. Packer, and Kyle Tousignant

ABSTRACT

A method was recently proposed, by Wei and Packer (2021), for application of the 2016 AISC *Specification* (AISC, 2016) to rectangular HSS sidewall instability. The proposal was based on evidence from prior research and collated data from international experiments. Herein, this topic is further updated with very recent research, and suggested improvements by others. An expanded database containing both experimental and numerical (finite element) tests of rectangular HSS-to-HSS cross connections with chord sidewall failure is hence amassed, totaling 227 tests. An analysis of this data reinforces the recent recommendations.

A review is given of methods in use for determining the structural reliability of steel members and connections. Based on this, a reliability study is performed on the recent recommendations, using various closed-form reliability methods as well as Monte Carlo simulation, to determine appropriate resistance factors for use with nominal-strength design equations for HSS sidewall instability. The influence of many variables, in particular chord sidewall slenderness, live-to-dead load ratio, as well as material and geometric properties, on the structural reliability of full-width rectangular HSS-to-HSS cross-connections under branch axial compression is studied.

KEYWORDS: hollow structural sections, cross connections, sidewall instability, reliability, resistance factors, Monte Carlo simulation.

INTRODUCTION

The 2016 AISC *Specification for Structural Steel Buildings* (AISC, 2016), hereafter referred to as the AISC *Specification*, provisions for web stability under local compression loading were applied to HSS connections by Wei and Packer (2021) through a limited experimental study and an analysis of a database of full-width rectangular HSS cross-connection experimental tests. This study showed that the web local crippling limit state never governs for HSS grades up to 50 ksi yield and sidewall slenderness values up to 57. Connections meeting the requirements do not need to be checked for web local crippling as a limit state. The web local yielding limit state in the AISC *Specification* was found to be very applicable to the full-width rectangular HSS cross (or X-) connection, illustrated in Figure 1.

Wei and Packer (2021) proposed to use the findings of Kuhn et al. (2019) to specify a limit for when the AISC *Specification* Chapter E can be used to determine the HSS chord sidewall (or web) compression buckling resistance. Instead of requiring the bearing length to be greater than the chord depth, as mentioned in the AISC *Specification* Commentary for I-shaped sections, a bearing length of greater than 0.25 of the chord depth was a more appropriate demarcation point for HSS connections (Kuhn et al., 2019). The effective length factor in the column buckling model is not stipulated by the *Specification* but was taken as 0.65 because rectangular HSS sidewalls resemble more of a fixed-fixed end restraint than a pin-pin end restraint. It was also determined that the branch angle of inclination, θ, does not have a definite impact on the cross-connection capacity; thus, the predicted cross-connection capacity (expressed as a force in an inclined branch) was conservatively limited to only the vertical force component of the branch member force (Wei and Packer, 2021). These proposals for applying the 2016 AISC *Specification* web compression limit states to rectangular HSS cross-connections are shown in Table 1. As with this current study, the connections were not susceptible to out-of-plane instability. With regard to Table 1 and thereafter, a list of symbol definitions is given at the end of the paper, but the symbols used herein are also in accord with the AISC *Specification*.

Dillon F. Rudman, WSP, Oakville, Ontario, Canada.
Email: dillon.rudman@wsp.com

Quanhan Xi, Department of Statistics, University of British Columbia, Vancouver, British Columbia, Canada. Email: johnny.xi@stat.ubc.ca

Jeffrey A. Packer, Department of Civil & Mineral Engineering, University of Toronto, Toronto, Ontario, Canada. Email: jeffrey.packer@utoronto.ca (corresponding)

Kyle Tousignant, Department of Civil & Resource Engineering, Dalhousie University, Halifax, Nova Scotia, Canada. Email: kyle.tousignant@dal.ca

Paper No. 2021-16

Table 1. Proposed Application of the 2016 AISC *Specification* Web Compression Limit States to Rectangular HSS Cross Connections, per Wei and Packer (2021)		
Limit State	**HSS-to-HSS Connection Nominal Strength, P_n (kips)**	**ϕ (Ω)**
Web local yielding, interior	For $l_{end} > H$ $2F_y t\left(7.5t+\frac{H_b}{\sin\theta}\right)$ (1)	1.00 (1.50)
Web local crippling, interior	For $l_{end} \geq H/2$ $1.6t^2\left(1+\frac{\frac{3H_b}{\sin\theta}}{H}\right)\sqrt{EF_y}Q_f$ (2)	0.75 (2.00)
Web compression buckling, interior, and $l_b \leq 0.25H$	For $l_{end} \geq H/2$ and $H_b/H\sin\theta \leq 0.25$ $\left(\frac{48t^3}{H-3t}\right)\sqrt{EF_y}Q_f$ (3)	0.90 (1.67)
Web compression buckling, interior, and $l_b > 0.25H$	For $l_{end} \geq H/2$ and $H_b/H\sin\theta > 0.25$ Use AISC *Specification* Equations E3-1, E3-2, and E3-3, with $K = 0.65$, L_c/r from Equation 4, and A_g (for each sidewall) from Equation 6	0.90 (1.67)

Fig. 1. Example of a full-width rectangular HSS cross connection, in vertical bracing.

For the web compression buckling limit state with $l_b > 0.25H$, the slenderness, λ or L_c/r, is calculated according to Equation 4 (Wei and Packer, 2021):

$$\lambda = \frac{KL}{r} = \frac{L_c}{r} = 3.46\left(\frac{H}{t} - 3\right)\sqrt{\frac{1}{\sin\theta}} \quad (4)$$

If the branch member is inclined, there is an allowance (indicated in Equation 4) resulting in a longer buckling length (Packer et al., 2009; IIW, 2012; ISO, 2013). A nondimensional slenderness, λ_C, can also be described by:

$$\lambda_C = \frac{\lambda}{\pi}\sqrt{\frac{F_y}{E}} \quad (5)$$

Using Equation 4, the critical stress, F_{cr}, can be determined for each chord sidewall or "column" from AISC *Specification* Section E3 and, using the cross-sectional area for each sidewall "column" (a load dispersion length multiplied by the wall thickness) given by Equation 6, the buckling strength of each sidewall can then be calculated.

$$A_g = \left(7.5t + \frac{H_b}{\sin\theta}\right)t \quad (6)$$

Herein, the topic of chord sidewall buckling in full-width rectangular HSS-to-HSS cross connections is further updated with recent research and suggested improvements by others. An evaluation of various failure models is conducted using data reflective of North American rectangular HSS strengths; a reliability study is then performed using various closed-form reliability methods, as well as Monte Carlo simulation (MCS), to determine appropriate resistance factors for use with the nominal-strength design equations recommended.

RECENT DEVELOPMENTS

Lan et al. (2021)

Recently, a review of competing proposals was performed by Wardenier et al. (2020) against a collated experimental and numerical database of full-width rectangular HSS-to-HSS cross connections in branch compression, which resulted in the following chord sidewall buckling equation, N_L (Lan et al., 2021):

$$N_L = C_f F_k (2H_b + 10t)\sqrt{\frac{1}{\sin\theta}}Q_f \quad (7)$$

where

$$F_k = \chi\left(\frac{H}{H_b}\right)^{0.15} F_y \le F_y \quad (8)$$

and

$$C_f = 1.1 - 0.1\frac{F_y}{355} \le 1.0 \quad (9)$$

The material factor (C_f in Equation 9, with F_y in MPa) was added to the proposed connection capacity by Lan et al. (2021) to cater for the influence of high-strength steels with a yield strength up to 139 ksi (960 Mpa). High-strength steel rectangular HSS connections have a larger elastic range, have material softening in the heat-affected zone, and are more prone than regular-strength steel rectangular HSS connections to production and fabrication imperfections (Lan et al., 2021). The branch angle effect of the proposed Equation 7 is in accordance with Davies and Roodbaraky (1987). Two possible methods were advocated for determining the buckling reduction factor χ: (1) using buckling curve c in EN 1993-1-1 (CEN, 2021), with a chord sidewall slenderness with an effective length factor of 0.5, and (2) a linear alternative given by:

$$\chi = 1.12 - 0.012\frac{H}{t}\sqrt{\frac{F_y}{355}} \le 1.0 \quad (10)$$

Despite the effort expended on achieving accurate nominal-strength models for the chord sidewall bucking limit state, in the format of Eurocode 3 (CEN, 2021), only a perfunctory reliability analysis was performed to obtain resistance expressions. Inclusion of the $(H/H_b)^{0.15}$ term in Equation 8 complicates the direct use of the AISC *Specification* Chapter E column buckling approach, so the method of Lan et al. (2021) is not considered further.

Kim and Lee (2021)

Kim and Lee (2021) performed a numerical and experimental study on rectangular HSS cross connections in which they proposed that, for full-width rectangular HSS cross connections, sidewall failure be idealized by a column model with a column width of H_b. Their proposed sidewall effective length factor, K, was variable, based on the branch and chord heights, as a value of 0.5 was found to be unconservative for high H_b/H. This variable K, with the corresponding width of the sidewall "column" based solely on H_b without any load dispersion, as shown in Equation 11, achieved better correlation with their database. The effect of branch angle was negligible; thus, it was neglected. The AISC-format connection strength equation for rectangular HSS cross-connection chord sidewall buckling under branch axial compression, with the Kim and Lee (2021) recommendations, N_{KL}, can be expressed by:

$$N_{KL} = 2F_{cr}tH_bQ_f \quad (11)$$

where F_{cr} is determined by AISC *Specification* Section E3,

Table 2. Database Limits Used in the Current Study		
Steel Nominal Yield Stress	**$2\gamma^*$ and 2γ Limit**	**l_b Limit**
≤70 ksi (483 MPa)	50.5	$H_b/H\sin\theta > 0.25$

with:

$$K = 0.5\sqrt{\frac{H_b}{H}} \tag{12}$$

DATABASE FOR FULL-WIDTH RECTANGULAR HSS CROSS-CONNECTION TESTS UNDER BRANCH COMPRESSION

As discussed previously, Wardenier et al. (2020) compiled an up-to-date database of recent tests, at the time, on rectangular HSS-to-HSS full-width cross connections with chord sidewall failure when subjected to branch compression [i.e., the database used by Lan et al. (2021)]. For the 51 experimental tests in that database, the source references of Fan (2017), Kuhn et al. (2019), Feldmann et al. (2016), and Pandey and Young (2020) were used. The latter two sources cover high-strength steel rectangular HSS connections with nominal yield strengths up to 139 ksi (960 Mpa)—far in excess of typical North American rectangular HSS strengths. The "numerical tests" (finite element models) included in the database were 21 by Yu (1997) and 152 by Kuhn (2018). In addition to other limits, Wardenier et al. (2020) screened their database to $2\gamma^* = H/t \le 40$ because no data was included for high-strength steel rectangular HSS connections with larger H/t. (Also, in general, rectangular HSS sections with large $2\gamma^*$ are sensitive to geometric imperfections.)

Recently, Wei and Packer (2021) and Kim et al. (2019) each completed two further tests on rectangular HSS full-width cross connections under axial compression, beyond the Wardenier et al. (2020) database. These four tests have been added, herein, to the experimental tests in the Wardenier et al. database to produce a new, extended experimental database (of 55 tests in total). Very recently, a further 48 numerical tests were generated by Kim and Lee (2021) to investigate chord sidewall failure of rectangular HSS cross-connections in compression. These numerical tests, in addition to those of Yu (1997) and Kuhn (2018), were compiled to produce a new, extended numerical database (of 221 tests in total).

To both the extended experimental and numerical databases, screening was applied by the authors. First, all tests with a yield strength greater than 70 ksi (483 Mpa) were removed because North American rectangular HSS strengths rarely exceed this. The $2\gamma^*$ and 2γ limit was increased from the value of 40 used by Wardenier et al. (2020) because data was available and high-yield HSS were not being considered. All tests with a bearing length less than 0.25 of the chord depth were also screened out to exclude tests failing by web (or sidewall) local yielding rather than sidewall buckling. (The limit state of sidewall local yielding is dealt with later in this paper.) Full data for the remaining 44 experimental and 183 numerical full-width rectangular HSS-to-HSS cross connections under branch axial compression from the extended database(s), which failed by chord sidewall buckling, are tabulated by Rudman (2021).

The parameter ranges for the experimental database are $\beta = 1.0$, $12.6 \le 2\gamma \le 42.2$, $12.6 \le 2\gamma^* \le 50.5$, $0.50 \le \eta \le 2.47$, $0.60 \le \eta^* \le 1.00$, $-0.87 \le n_0 \le 0$, $44° \le \theta \le 90°$, and 33 ksi (228 Mpa) $\le F_y \le$ 70 ksi (483 Mpa). The 44 experimental rectangular HSS sections were either cold formed or hot finished; 14 have a non-90° angle, while the other 30 tests have a 90° angle. The parameter ranges for the numerical database are $\beta = 1.0$, $10 \le 2\gamma \le 35$, $10 \le 2\gamma^* \le 35$, $0.25 \le \eta \le 2.00$, $0.21 \le \eta^* \le 2.50$, $-0.80 \le n_0 \le 0.75$, $\theta = 90°$, and 49 ksi (338 Mpa) $\le F_y \le$ 70 ksi (483 Mpa). The 183 numerical rectangular HSS sections were either cold formed or hot finished. The prime limits of the screened database are shown in Table 2.

EVALUATION OF DESIGN PROPOSALS

The compiled and screened database was evaluated against the following design methods for sidewall buckling failure in rectangular HSS-to-HSS cross connections under branch axial compression:

1. AISC *Specification* Chapter J, assuming Chapter E is applied for $l_b > H$, and (a) $K = 1.0$; (b) $K = 0.65$.
2. Wei and Packer (2021) proposal, assuming Chapter E is applied for $l_b > 0.25H$, and $K = 0.65$.
3. Kim and Lee (2021) recommendations.

For the combined database of 227 tests on full-width rectangular HSS-to-HSS cross-connection tests under branch axial compression, the resulting statistical evaluation of various design methods for chord sidewall buckling is shown in Figure 2. The mean and coefficient of variation (COV) of the ratios N_{1u}/N_{AISC}, N_{1u}/N_{WP}, and N_{1u}/N_{KL} are indicated on the plots, where N_{1u} represents the connection ultimate strength and N_{AISC}, N_{WP}, and N_{KL} represent nominal strength prediction models. It can be seen that all methods feature

over- and underestimations of the ultimate strength. Figures 2(a) and 2(b) show correlations by applying the provisions of AISC *Specification* Chapter J to HSS and using the Chapter E column buckling approach for bearing lengths $l_b > H$. Regardless of the effective length factor used [K = 1.0 in Figure 2(a); K = 0.65 in Figure 2(b)], the COV is high, reflecting an imprecise model.

The Kim and Lee (2021) equation, Figure 2(d), consistently underpredicts the strength of connections with a low sidewall slenderness and produces the largest mean ratio. This can be attributed to their proposed change to the width of the sidewall "column." In low-slenderness HSS, the sidewall thickness adds a significant amount of width to the bearing length (due to load dispersion). Eliminating this width from the nominal-strength equation results in underpredicting connection strength. As the sidewall slenderness increases, the wall thickness contributes less to the width of the failure area, and the connection strength predictions

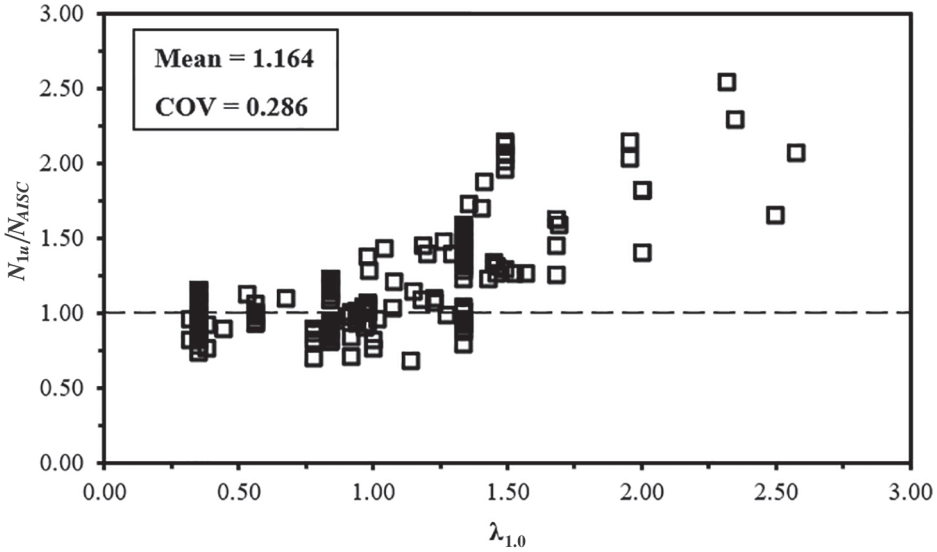

(a) 2016 AISC Specification *Chapter J, Chapter E is applied for* $l_b > H$*, and using* $K = 1.0$

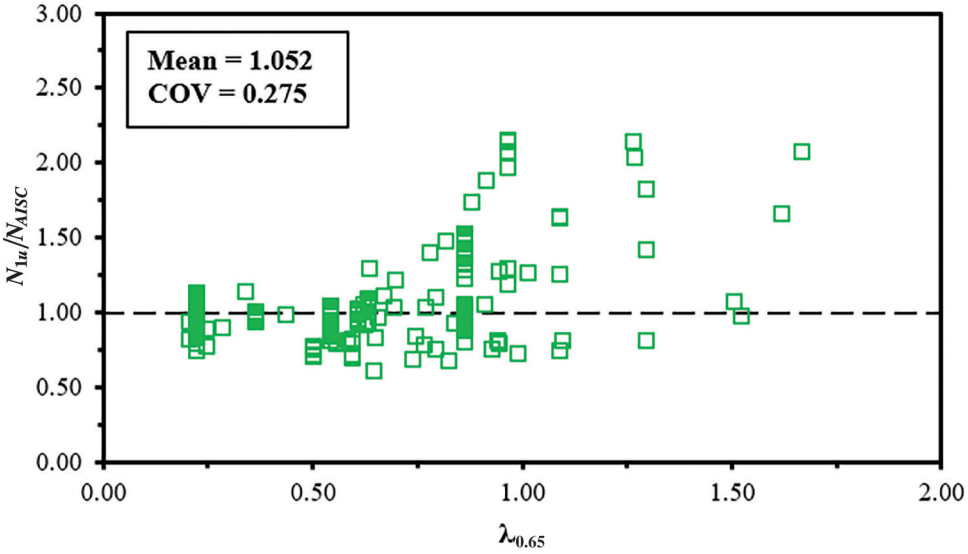

(b) 2016 AISC Specification *Chapter J, Chapter E is applied for* $l_b > H$*, and using* $K = 0.65$

Fig. 2(a-b). Comparison of 227 rectangular HSS-to-HSS cross-connection test results against prediction methods.

using the Kim and Lee (2021) equation become more accurate. This results in their proposed design equation producing a large COV and thus being an imprecise predictor of the connection strength.

The Wei and Packer (2021) proposed design method, Figure 2(c), produces the lowest actual-to-predicted mean ratio; however, it is still greater than 1.0. Significantly, it has a much lower COV than the other design models considered. Thus, the Wei and Packer (2021) proposal for HSS chord sidewall buckling (Table 1) is still recommended for adoption. The following sections of this paper deal with determining the appropriate resistance factor, ϕ, for use with this design approach.

STRUCTURAL RELIABILITY, TARGET RELIABILITY INDEX, AND RESISTANCE FACTORS

It is well-known that engineering decisions must be made in the presence of uncertainties arising from inherent

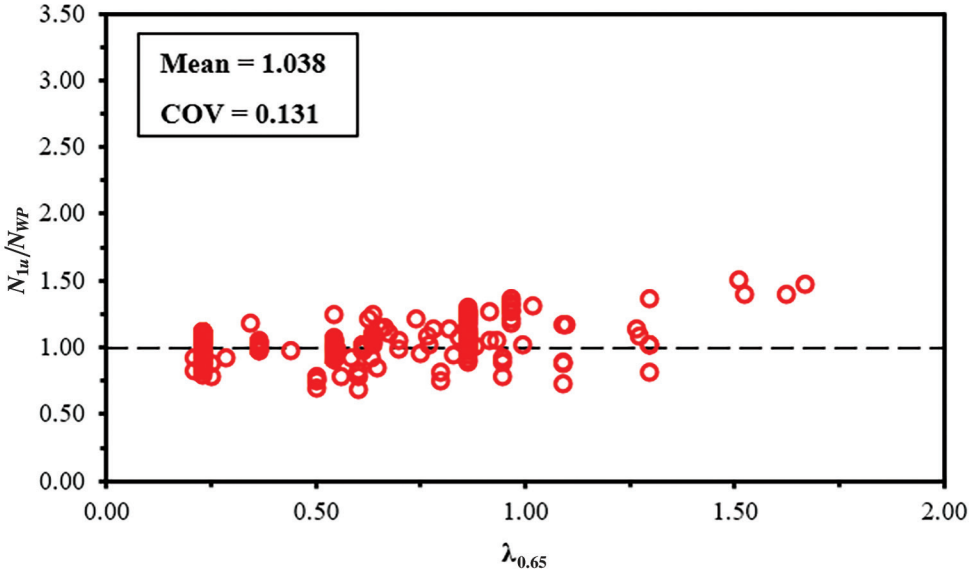

(c) Wei and Packer (2021) proposal, Chapter E is applied for $l_b > 0.25H$*, and using* $K = 0.65$

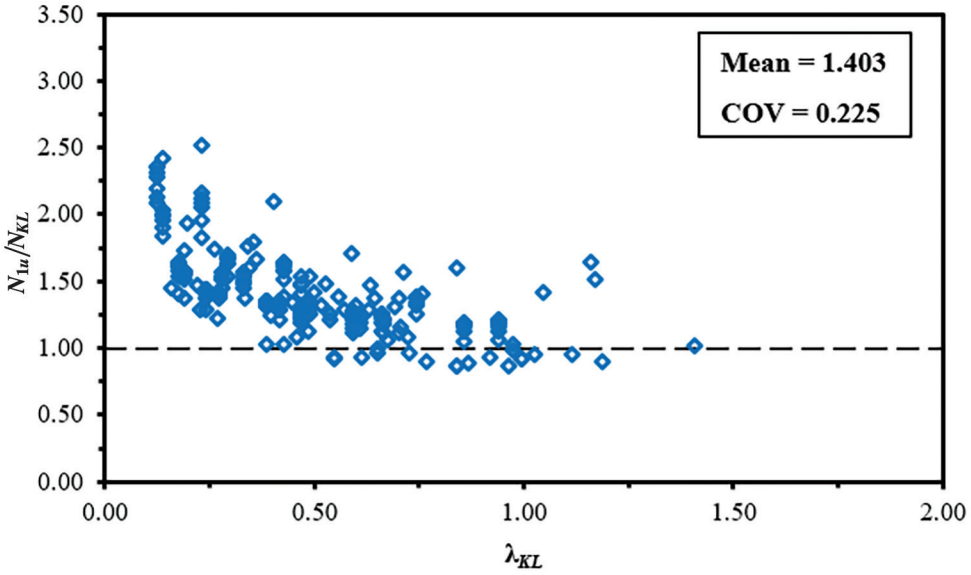

(d) Kim and Lee (2021) proposal with variable K

Fig. 2(c-d). Comparison of 227 rectangular HSS-to-HSS cross-connection test results against prediction methods.

randomness in design parameters and imperfect modeling. Due to these uncertainties, potential risk arises in engineering design; therefore, safety factors are required to ensure an acceptable level of risk, and absolute reliability is an unattainable goal because of uncertainties (Ellingwood et al., 1980).

The structural reliability of a member or element is based on the limit state where the member's resistance, R, and the load effect, S, acting on the member are compared (Melchers and Beck, 2018). A failure event occurs under the following conditions, or any other equivalent criteria:

$$R - S < 0 \qquad \frac{R}{S} < 1 \qquad \ln(R) - \ln(S) < 0 \tag{13}$$

The randomness in the resistance of an element, R, and the load effect, S, can be accounted for by introducing dimensionless random variables. For the resistance, these random variables help account for variations in the properties of the element and the assumptions used in determining the resistance (Ravindra and Galambos, 1978). For the load effect, the random variables account for uncertainties in load intensities and structural analysis (Ravindra and Galambos, 1978). The random variable obtained by subtracting ln(S) from ln(R), is called the safety margin, g:

$$g = \ln(R) - \ln(S) = \ln(R/S) \tag{14}$$

and the probability of failure, p_F, of a structural element can thus be represented by:

$$p_F = P\left[g < 0\right] \tag{15}$$

The probability distribution of g is unknown in practice. However, if the assumption is made that R and S are independently log-normally distributed, then g is normally distributed, and a first-order probabilistic method requiring only the mean and standard deviation may be used (Ravindra and Galambos, 1978). These parameters may be summarized into a relative measure of safety, known as the safety index, β^+, defined as follows (Ellingwood et al., 1980):

$$\beta^+ = \frac{g_m}{\sigma_g} \tag{16}$$

where g_m is the mean value of g and σ_g is the standard deviation of g. The reliability index can be conveniently interpreted as the distance from the mean to the origin, representing failure, in units of standard deviations. Substituting the expression in Equation 14 results in:

$$\beta^+ = \frac{\left[\ln\left(\frac{R}{S}\right)\right]_m}{\sigma_{\ln\left(R/S\right)}} \tag{17}$$

and Equation 17 may be approximated using first-order statistics of R and S:

$$\beta^+ \simeq \frac{\ln\left(\frac{R_m}{S_m}\right)}{\sqrt{V_R^2 + V_S^2}} \tag{18}$$

where R_m and S_m are the means of the resistance and load effect and V_R and V_S are the corresponding COVs. Equation 18 includes a small-variance approximation [i.e., substitutions for $\ln(R/S)_m$ and $\sigma_{\ln(R/S)}$] that are valid when V_R and V_S are both less than about 0.30 (Ellingwood et al. 1980). If this condition is violated, β^+ can instead be determined by using Equation 19, which is exact if R and S are assumed to be independent log-normal random variables (Benjamin and Cornell (1970),

$$\beta^+ = \frac{\ln\left(\frac{R_m}{S_m}\sqrt{\frac{1+V_S^2}{1+V_R^2}}\right)}{\sqrt{\ln\left[(1+V_S^2)(1+V_R^2)\right]}} \tag{19}$$

In either case, the probability of failure, p_F, may be computed as:

$$p_F = \Phi\left[-\beta^+\right] \tag{20}$$

If R and S are instead described by independent normal distributions, a more appropriate formulation for the safety margin is:

$$g = R - S \tag{21}$$

In addition,

$$\beta^+ = \frac{R_m - S_m}{\sqrt{\sigma_R^2 + \sigma_S^2}} \tag{22}$$

and substitution of Equation 22 into Equation 20 for p_F yields an exact probability of failure.

The resistance of a structural steel member or connection, R, is often assumed to be a function of the material strength, the geometric properties, and a professional factor. The professional factor accounts for the imperfect nominal resistance design equation. Typically, these relationships are further assumed to be represented by actual-to-nominal ratios in the form:

$$R = MGPR_n \tag{23}$$

The material ratio, M, is the ratio of the actual-to-nominal relevant material property of the structural steel. The geometric ratio, G, is the ratio of the actual-to-nominal relevant geometric properties of the structural steel. The professional ratio, P, represents the ratio of observed capacity in tests (experimental or numerical) to predicted capacity,

with the latter based on measured material and geometric properties and a nominal strength model, R_n.

Similarly, the load effects on a steel member or connection can be assumed to be represented by the sum of the actual-to-nominal ratios for the applied loads and their nominal value. The load effect, S, can hence be written as:

$$S = \sum \delta_{S,i} S_{n,i} \tag{24}$$

where δ_S is the actual-to-nominal ratio for a load effect and S_n is the nominal load effect. The subscript i refers to the load effect under consideration (dead, live, etc.).

Load and resistance factor design (LRFD) and limit states design (LSD) criteria are based on an expression where the resistance of an element must be greater than the sum of the factored load effects acting on the element; that is,

$$\phi R_n \geq \sum_{i=1}^{j} \alpha_i S_{n,i} \tag{25}$$

The resistance side of the criterion is the product of the nominal resistance of the element, R_n, and a dimensionless resistance factor, ϕ. The load effect side of the criterion is the sum of the products between the various nominal load effects, S_n, and the associated dimensionless load factor, α_i.

Separation Factor Approach

Equation 18 can be rearranged and expressed as a first-order probabilistic design criterion with a central safety factor, θ_C (Ravindra and Galambos, 1978), which combines the uncertainties of both the resistance and load effects; that is,

$$R_m \geq \theta_C S_m \tag{26}$$

$$\theta_C = e^{\left(\beta^+ \sqrt{V_R^2 + V_S^2}\right)} \tag{27}$$

Lind (1971) proposed the following linear approximation, Equation 28, to the square root of the sum of squares terms in the exponent of Equation 27, which allows for the separation of the resistance and load effect terms. In doing so, the resistance factor can be determined without knowledge of the load effects (and load factors can be determined without knowledge of the resistance). For a range of $⅓ \leq V_R/V_S \leq 3$, with $\alpha = 0.75$ (where α is the coefficient of separation), this approximation is within about 6%. Equation 29 is established through substitution of Equation 28 into Equations 27 and 26.

$$\sqrt{V_R^2 + V_S^2} = \alpha(V_R + V_S) \tag{28}$$

$$e^{\left(-\alpha\beta^+ V_R\right)} R_m \geq e^{\left(\alpha\beta^+ V_S\right)} S_m \tag{29}$$

Galambos and Ravindra (1973) extended this concept further by introducing two different separation factors, one for the load effects, and one for the resistance. They went on to show that a value of $\alpha = 0.55$ on the resistance side of the equation gave a near-zero error and a standard deviation of 3% for a limited range of key variables. This was determined through an error minimization process considering combinations of dead, live, and wind load (Galambos and Ravindra, 1977). After the addition of random variables and linear approximations to the LRFD criterion, the resistance factor can be expressed as seen in Equation 30 (Ravindra and Galambos, 1978).

$$\phi = \frac{R_m}{R_n} e^{\left(-\alpha\beta^+ V_R\right)} \tag{30}$$

The value of β^+ was determined by selecting a standard design situation with the allowable stress design method and requiring that the LRFD criterion generally produce the same element to resist the forces. For structural elements, $\beta^+ = 3.0$, while for structural connectors, $\beta^+ = 4.5$ (Ravindra and Galambos, 1978).

Many past studies have taken R_m/R_n to simply be the ratio of observed capacity in tests (experimental or numerical) to predicted capacity, with the latter based on measured material and geometric properties and a nominal strength model. Therefore, V_R is also simply taken as the COV of the observed capacity in tests (experimental or numerical) to predicted capacity. The "separation factor approach" used throughout this study adopts this methodology, with a separation factor of $\alpha = 0.55$ in accordance with Ravindra and Galambos (1978). As noted earlier, a value of $\alpha = 0.75$ (Lind, 1971) has also been used, historically, with ACSE (2016) currently advocating for a value of $\alpha \approx 0.70$.

Expanded Separation Factor Approach

If M, G, and P are assumed to be independently log-normal, then the mean resistance, R_m, can be expressed using the ratio of mean to nominal resistance, δ_R:

$$R_m = \delta_R R_n \tag{31}$$

where

$$\delta_R = \delta_M \delta_G \delta_P \tag{32}$$

and δ_M, δ_G, and δ_P represent the mean values for M, G, and P, respectively. The COV of the resistance is well approximated by the square root of the sum of the squares of the three different COVs—V_M, V_G, and V_P—which are associated with δ_M, δ_G, and δ_P. The resistance factor equation can be seen in Equation 34.

$$V_R = \sqrt{V_M^2 + V_G^2 + V_P^2} \tag{33}$$

$$\phi = \delta_R e^{\left(-\alpha\beta^+ V_R\right)} \tag{34}$$

This approach applies to members whose resistance is a direct product of a geometric and material property. For

members, whose resistance is a product of many geometric and material properties, the contribution from each property must be determined over the range of the independent variable. The relative contribution of each of the distinct properties to the mean ratios and the related COVs can be approximated by mathematical manipulation of the resistance equation, using a partial derivative approach (Kennedy and Gad Aly, 1980). Depending on how the equation describing the property was determined, either on a solely mathematical basis or a semi-empirical or curve-fitting basis, different participation factors for the various properties will be determined (Kennedy and Gad Aly, 1980).

Effect of Material Parameters

The resistance of a structural steel column under compression loading is governed by its overall slenderness, which determines the critical buckling stress, which, in turn, depends on the radius of gyration (a geometric parameter), the yield stress, and the modulus of elasticity (material parameters). Thus, as the column slenderness varies, so does the dependency on the material parameters. Schmidt and Bartlett (2002) showed that for columns, using the overall flexural buckling equation in CSA S16 (CSA, 2019a), at low slenderness the yield strength contributes more to the material mean ratio and COV, while at high slenderness the radius of gyration and modulus of elasticity dominate. Because statistical parameters for materials are contingent on column slenderness, different resistance factors are therefore determined for various chord sidewall slenderness values. This results in a range of resistance factors (or alternatively safety indices) for rectangular HSS sidewalls under branch compression.

Lognormality of the Resistance

Equations 23 and 32 are convenient due to the log-normality assumption. When the material strength, geometric properties, and professional factor are independently log-normal, so is the resistance. A log-normal distribution can be described entirely through its mean and COV (second-order statistical parameters). If the log-normality assumption is true, then the probability of failure, or reliability index, can be determined through the mean and COVs of material strength, geometric properties, and professional factor. Reliability analysis techniques make this assumption in order to predict the probability of failure, or reliability index, using second-order statistical parameters from survey and test data. In a recent paper by Xi and Packer (2021), this assumption was assessed for the resistance.

The data for actual-to-predicted nominal strength (professional factor) that are obtained from experimental or numerical tests are often a poor fit to normal or log-normal probability distributions. The typical data for actual-to-nominal distributions of the material and geometric properties of HSS sections are generally a reasonable fit to normal or log-normal probability distributions. When all the data is combined, the resistance distribution has a more regular shape (Xi and Packer, 2021). Xi and Packer used actual-to-nominal data of the material strength from Liu (2016) and actual-to-nominal data of the geometric properties from Kennedy and Gad Aly (1980), as well as actual-to-predicted test data from rectangular HSS-to-HSS cross connections with chord sidewall failure from Wei and Packer (2021) and Bu et al. (2021). It was shown that the combined resistance obtained by a simulation procedure closely approximated a log-normal distribution even if some of the data was seemingly incompatible (Xi and Packer, 2021). Despite having an irregular distribution for the professional factor, the expanded separation factor approach can be used for evaluating the reliability of HSS connections.

As an example of this effect, Figure 3(a) shows the actual-to-predicted ultimate strength correlation for the limit state of web buckling, using the method of Wei and Packer (2021) and the experimental data for full-width HSS cross connections from that paper. After sampling from this professional factor histogram, plus typical distributions for material and geometric properties, the numerically simulated resistance (using 1.9 million samples) is shown in Figure 3(b). The continuous curve (red line) represents the best-fit log-normal distribution using an iterative maximum likelihood estimation (MLE) technique. The statistical parameters given in Figure 3 pertain to the histograms.

Approximate FORM Approach

Nowak and Lind (1979) showed that the load side of the LRFD inequality (Equation 25) can be considered in determining the resistance factor (or, alternatively, the reliability index) by using the following equation:

$$\phi = \delta_R \frac{\sum \alpha_i S_{n,i}}{S_m} e^{\left[-\beta^+\left(V_R^2+V_S^2\right)^{1/2}\right]} \tag{35}$$

The most accurate results for this first-order reliability method (FORM) occur when both the resistance and load side of the LRFD reliability inequality have a log-normal distribution. Of late, it has become common practice to consider the load side of the LRFD reliability inequality when determining resistance factors, and it is even stipulated by some standards such as CSA S408-11 (CSA, 2011). Considering only the basic combination of dead and live loads, Schmidt and Bartlett (2002) determined the following expressions for the reliability index and resistance factor:

$$\beta^{+} = \frac{1}{\sqrt{V_R^2 + V_S^2}} \ln\left\{\frac{\delta_R}{\phi}\left[\frac{\alpha_D + \alpha_L\left(L/D\right)}{\delta_D + \delta_L\left(L/D\right)}\right]\right\} \quad (36)$$

$$\phi = \delta_R\left[\frac{\alpha_D + \alpha_L\left(L/D\right)}{\delta_D + \delta_L\left(L/D\right)}\right] e^{\left(-\beta^{+}\sqrt{V_R^2 + V_S^2}\right)} \quad (37)$$

where δ_R is the mean ratio of the resistance and is comprised of three different mean ratios in accordance with the expanded separation factor approach, V_R is the COV of the resistance per the expanded separation factor approach, V_S is the COV of the load effects, α_D and α_L are the load factors for dead and live loads, δ_D and δ_L are the bias coefficients for dead and live loads, and L/D is the live-to-dead load ratio. Only the combination of dead and live loads is considered in this paper.

Schmidt and Bartlett (2002) also computed the resistance factor over a range of L/D ratios. This results in a range of reliability indices for a particular structural steel member (or connection). The load effect was assumed to have a log-normal distribution because the L/D ratio for steel members typically exceeds 1.0, thus the log-normal live load distribution component dominates the load effect (Schmidt and Bartlett, 2002). Galambos (2006) has also used both the load side of the LRFD reliability inequality and the L/D ratio to determine resistance factors.

Reliability Method of CSA S408-11

The Canadian Standards Association provides a standard, CSA S408-11 (CSA, 2011), with guidelines for the development of limit states design standards. Annex B.2.5 of CSA S408-11 provides a so-called Approximate Method (an approximate FORM) for calculating the resistance factor to achieve target reliability values for arbitrary limit states. Annex B.2.5 cites Equation 35, which is to be used with load factors and load combinations specified in a loading standard such as NBC (2020) or ASCE (2016). Applying the

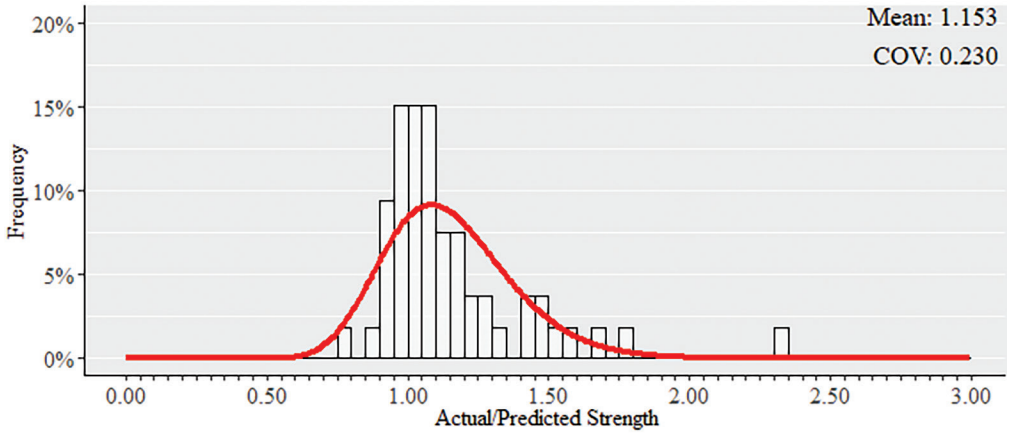

(a) Statistical correlation for professional factor only

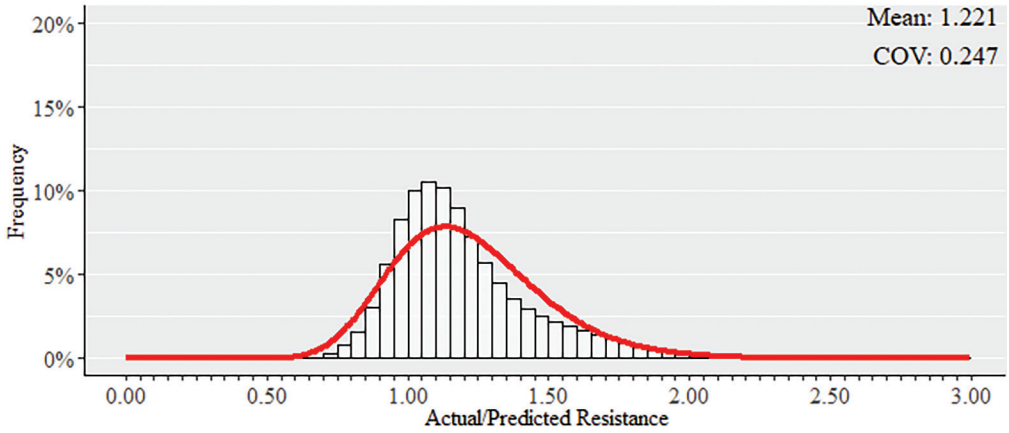

(b) Statistical correlation for numerically simulated resistance

Fig. 3. Resistance smoothing effect produced by sampling from multiple histograms (Xi and Packer, 2021).

basic dead plus live load combination to the approximate FORM analysis, and expressing the equation as a function of the L/D ratio, gives the resistance factor in Equation 37. Annex B.2.5 of CSA S408-11 states that the COV of the load effects can be determined by Clause 14.15.2.3 of CSA S6:19 (CSA, 2019b), which is given by Equation 38 for dead plus live load.

$$V_S = \frac{\sqrt{(\delta_D V_D)^2 + \left[\delta_L V_L \left(L/D\right)\right]^2}}{\delta_D + \delta_L \left(L/D\right)} \tag{38}$$

Reliability Method of AISI S100-16

Chapter K of American Iron and Steel Institute S100-16 (AISI, 2016) provides a method to determine the resistance factor of a cold-formed structural steel resistance equation by direct testing. This method uses the LRFD criterion to determine the resistance factor but simplifies the load side to a single load combination ($1.2D + 1.6L$) and $L/D = 5$ (Meimand and Schafer, 2014). The resistance factor given by AISI S100, Section K2.1.1 (AISI, 2016) is in an "expanded separation factor" form:

$$\phi = C_\phi (\delta_M \delta_G \delta_P) e^{-\beta^+ \sqrt{V_M^2 + V_G^2 + C_P V_P^2 + V_S^2}} \tag{39}$$

where C_ϕ is a calibration coefficient and C_P is a correction factor for sample size. For the material factor and the fabrication factor, the means (δ_M and δ_G, respectively) are to be determined from statistical analysis but are not to be greater than the values given in Table K2.1.1-1, while the COVs (V_M and V_G, respectively) are not to be less than the values given in Table K2.1.1-1 (AISI, 2016). The calibration coefficient, target safety index, and COV for the load effects are predetermined factors based on LRFD criteria, with the mean value of the professional factor given by:

$$\delta_P = \frac{\sum_{i=1}^{n_t} \frac{R_{t,i}}{R_{n,i}}}{n_t} \tag{40}$$

where n_t is the number of tests, R_t is the tested strength, and R_n is the nominal strength by a rational engineering analysis. The subscript i denotes an individual test within a series of tests. The correction factor for sample size is given by:

$$C_P = \frac{\left(1 + \frac{1}{n_t}\right) m}{m - 2} \tag{41}$$

where m is the number of degrees of freedom ($m = n_t - 1$). The COV for the test results is given by:

$$V_P = \frac{\sigma_P}{\delta_P} \tag{42}$$

where σ_P is the standard deviation of the ratio of actual-to-nominal strengths.

Monte Carlo Simulation Approach

As yet another alternative to the previous approaches, Monte Carlo techniques can be used to randomly sample from the various resistance and load effect parameter distributions to determine a possible resistance and load effect scenario for a member or connection. This process closely approximates the probabilistic behavior of the resistance and load effect for the desired design scenario with a large number of samples. This sampling technique is known as a Monte Carlo simulation (MCS). Kennedy and Baker (1984), Lundberg and Galambos (1996), Hong and Zhou (1999), and others have undertaken such MCSs. MCS is also advocated as a reliability analysis method in some codes and standards (e.g., CSA S408-11).

RESISTANCE FACTOR EVALUATION FOR WEI AND PACKER (2021)

In this study, statistical parameters were taken as $\delta_D = 1.05$ and $V_D = 0.10$ for the dead load effect and as $\delta_L = 0.78$ and $V_L = 0.32$ for the live load effect (Schmidt and Bartlett, 2002). Dead loads can be more accurately predicted than live loads, and for comparison, values of $\delta_D = 1.0$ and $V_D = 0.08$ were used in a previous reliability study of tubular connections in offshore structures (Packer and Kremer, 1988). Values of $\alpha_D = 1.20$ and $\alpha_L = 1.60$ were used, per ASCE/SEI 7-16 (ASCE, 2016), and material statistical parameters of $\delta_M = 1.178$ and $V_M = 0.086$ per Xi and Packer (2021). These material parameters are based on a survey done by Liu (2016) on variations in yield stress of A500 (ASTM, 2021) dual-certified Grade B/C rectangular HSS. The geometric statistical parameters, $\delta_G = 0.975$ and $V_G = 0.025$, were adopted from a survey by Kennedy and Gad Aly (1980), but the proposed design method depends on multiple rectangular HSS geometric properties, such as chord thickness and height. The geometric statistical parameters taken in this study are the lowest mean ratio and the highest COV, from all the contributing properties, to be conservative. The target safety index, β^+, for the ductile connections under consideration was assigned to be 3.0, which is in accord with the Commentary to 2016 AISC *Specification* Section B3.1. A target safety index of 3.0 is now a commonly accepted level of safety for public buildings, corresponding to a notional probability of structural failure of 1.35×10^{-3} (Packer and Kremer, 1988).

For the AISI S100-16 reliability method, the material and geometric statistical parameters were compared with the requirements in Chapter K of that specification. The only statistical parameter that was in accordance with the requirements was the geometric ratio (mean). The other statistical

parameters were hence taken from Table K2.1.1-1. The calibration coefficient and COV for the load effect were taken as $C_\phi = 1.52$ and $V_S = 0.21$, respectively, due to use of the LRFD format (AISI, 2016). The target reliability index, β^+, was assigned to be 2.5 because the connection resistance is dependent on the HSS members and the use of the LRFD equation (AISI, 2016).

The professional factor statistical parameters used for the Wei and Packer (2021) proposed approach for the chord sidewall compression buckling limit state are taken from the results of the combined database: $\delta_P = 1.038$ and $V_P = 0.131$ [see Figure 2(b)]. (The professional factors from the experimental and numerical databases, separately, are similar to the combined values.)

SIDEWALL COMPRESSION BUCKLING

Closed-Form Solutions

The resistance factor for chord sidewall compression buckling can be determined by the various closed-form methods. Two different sets of material statistical parameters can be used to determine the resistance factors: (1) parameters based only on the yield stress and (2) parameters that depend on the chord sidewall slenderness.

Based on Chord Yield Stress

Using the previously noted material statistical parameters for yield stress, the resistance factor is 0.836 for the separation factor approach and 0.917 for the expanded separation factor approach. The resistance factors over a range of L/D ratios, using the approximate FORM analysis in CSA S408-11, can be seen in Figure 4, wherein the dip at a L/D ratio of about 0.2 is due to the intersection of the two factored load combinations from ASCE/SEI 7 (ASCE, 2016): $1.4D$ (dead load only) and $1.2D + 1.6L$. By equating these two loading situations with mean loads, one obtains $(L/D) = 0.168$. The resistance factor using the AISI S100-16 approach is 0.857.

Based on Chord Sidewall Slenderness

A mathematical manipulation of the equations describing the critical yield stress for columns in axial compression was performed to determine the relative contribution of each distinct property to the material statistical parameters. The material statistical parameters depend on the yield stress, radius of gyration (which in turn depends on the thickness), and modulus of elasticity. The statistical parameters were taken as $\delta_r = 0.975$ and $V_r = 0.025$ for radius of gyration and $\delta_E = 1.000$ and $V_E = 0.019$ for modulus of elasticity, from Kennedy and Gad Aly (1980). Although δ_M and V_M can be shown to vary with the chord sidewall slenderness, material statistical parameters at the average chord sidewall slenderness of the combined database were chosen to determine the resistance factors for the various methods. The average slenderness of the database is 0.619, which results in $\delta_M = 1.134$ and $V_M = 0.070$.

For the separation factor approach, these material statistical parameters do not change the resistance factor determined previously because the separation factor approach (as used herein) is based on only the professional factor parameters. The expanded separation factor approach, on

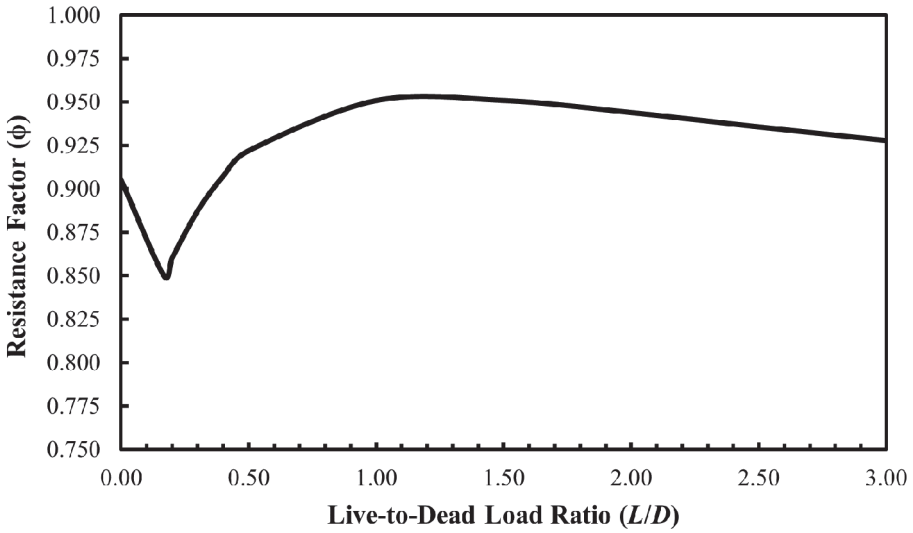

Fig. 4. Resistance factor for the Wei and Packer (2021) proposed buckling method, using the approximate FORM analysis in CSA S408-11, with material statistical parameters based on yield stress.

the other hand, produces a resistance factor of 0.894 (compared to 0.917 previously). For the approximate FORM analysis in CSA S408-11, the resistance factors over a range of L/D values are shown in Figure 5 and these can be seen to be lower than those in Figure 4, and for the AISI S100-16 reliability method, statistical parameters based on chord sidewall slenderness do not meet the material requirements of Chapter K; thus, the resistance factor is retained as the one determined with just the yield stress (0.857).

Participating Variables for MCS

As can be seen in Table 1, the participating random variables in the Wei and Packer (2021) method for sidewall compression buckling resistance are the material strength (yield stress), modulus of elasticity, chord thickness, chord height, branch height, and the professional factor.

Material strength variations for ASTM A500 dual-certified Grade B/C rectangular HSS compiled by Liu (2016) were used (Figure 6), from which the raw data (n_t = 3018) was obtained. The continuous curve (red line) in Figure 6, and subsequent histograms for variables, represents the best-fit log-normal distribution using the aforementioned iterative MLE technique. Statistical parameters given in the figures pertain to the histograms.

For modulus of elasticity, the variation determined by Galambos and Ravindra (1978) was used. A log-normal distribution was created (on the basis of its limitation to

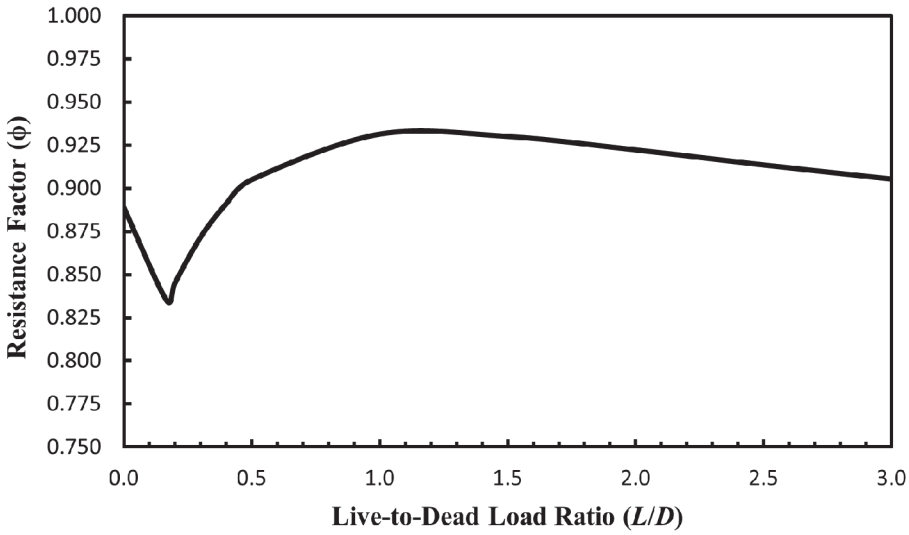

Fig. 5. Resistance factor for the Wei and Packer (2021) proposed buckling method, using the approximate FORM analysis in CSA S408-11, with material statistical parameters based on chord sidewall slenderness.

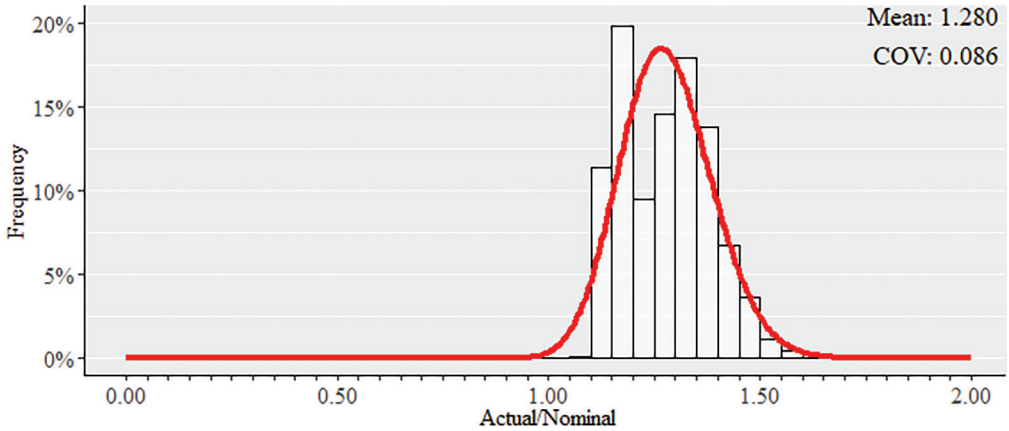

Fig. 6. ASTM A500 dual-certified Grade B/C rectangular HSS yield stress variation (Liu, 2016).

Table 3. Representative Connections for Monte Carlo Simulation								
Connection Number	Chord Member $H \times B \times t$	Branch Member $H_b \times B_b \times t_b$	H (in.)	t (in.)	H_b (in.)	θ (°)	$H_b/H\sin\theta$	H/t
1	6×6×⅜	3×6×⅜	6.00	0.349	3.00	90	0.50	17.2
2	6×6×⅜	6×6×⅜	6.00	0.349	6.00	90	1.00	17.2
3	6×6×⅜	12×6×⅜	6.00	0.349	12.0	90	2.00	17.2
4	6×6×⅜	12×6×⅜	6.00	0.349	12.0	60	2.31	17.2
5	6×6×⅜	12×6×⅜	6.00	0.349	12.0	45	2.83	17.2
6	8×8×⅜	4×8×⅜	8.00	0.349	4.00	90	0.50	22.9
7	8×8×⅜	8×8×⅜	8.00	0.349	8.00	90	1.00	22.9
8	8×8×⅜	12×8×⅜	8.00	0.349	12.0	90	1.50	22.9
9	8×8×⅜	8×8×⅜	8.00	0.349	8.00	60	1.16	22.9
10	8×8×⅜	8×8×⅜	8.00	0.349	8.00	45	1.41	22.9
11	12×12×⅜	12×4×⅜	12.0	0.349	4.00	90	0.33	34.4
12	12×12×⅜	12×6×⅜	12.0	0.349	6.00	90	0.50	34.4
13	12×12×⅜	12×8×⅜	12.0	0.349	8.00	90	0.67	34.4
14	12×12×⅜	12×12×⅜	12.0	0.349	12.0	90	1.00	34.4
15	12×12×⅜	12×12×⅜	12.0	0.349	12.0	60	1.16	34.4
16	12×12×⅜	12×12×⅜	12.0	0.349	12.0	45	1.41	34.4
17	16×16×⅜	16×8×⅜	16.0	0.349	8.00	90	0.50	45.8
18	16×16×⅜	16×12×⅜	16.0	0.349	12.0	90	0.67	45.8
19	16×16×⅜	16×16×⅜	16.0	0.349	16.0	90	1.00	45.8

a non-negative value) from the statistical parameters in Galambos and Ravindra (1978). Samples were then taken from this log-normal distribution.

Geometric variations were determined through the surveys of Kennedy and Gad Aly (1980). The raw data for the rectangular HSS thickness (n_t = 302) and height (n_t = 149) surveys could not be obtained, so sampling was performed directly from the histograms. The sampling procedure followed was to select a histogram bin with probability proportional to its reported frequency, then to simulate a value uniformly within the limits of the bin (Xi and Packer, 2021). Figures 7 and 8 show the geometric variations used.

Professional factor variations were obtained from the combined database compiled herein by comparing the actual connection strength with the nominal strength predicted by Wei and Packer (2021). Sampling was thus performed from the histogram in Figure 9. Professional factors were not binned into various combinations (by branch angle, chord sidewall slenderness, and bearing length) as the number of tests within each bin would, in that case, be too minimal.

For the load effect, variations in dead load generally resemble a normal distribution (Ellingwood et al., 1980), whereas variations in live load can generally be described by a Gumbel distribution (Ellingwood and Culver, 1977). Herein, an equivalent log-normal distribution for the variations of dead load was created, per Ellingwood et al., based on the statistical parameters for normal distribution given in Schmidt and Bartlett (2002). For the live load, an equivalent log-normal distribution, as derived by Schmidt and Bartlett, has been used. Samples were then taken from these distributions.

MCS Method

A representative set of 19 full-width (β = 1.0) connections, listed in Table 3, was formulated for rectangular HSS-to-HSS axially loaded cross connections, covering the parametric range of $17.2 \le 2\gamma^* \le 45.8$, $0.33 \le H_b/H\sin\theta \le 2.83$, and $45° \le \theta \le 90°$. A nominal yield stress, F_y, of 50 ksi (345 MPa) was used. A reliability index was determined using Equation 16 for each one of the representative connections, using a given resistance factor and a particular L/D ratio, by sampling 1 million times from the participating variable distributions. Details of the sampling method, using MATLAB, can be found in Rudman (2021). This

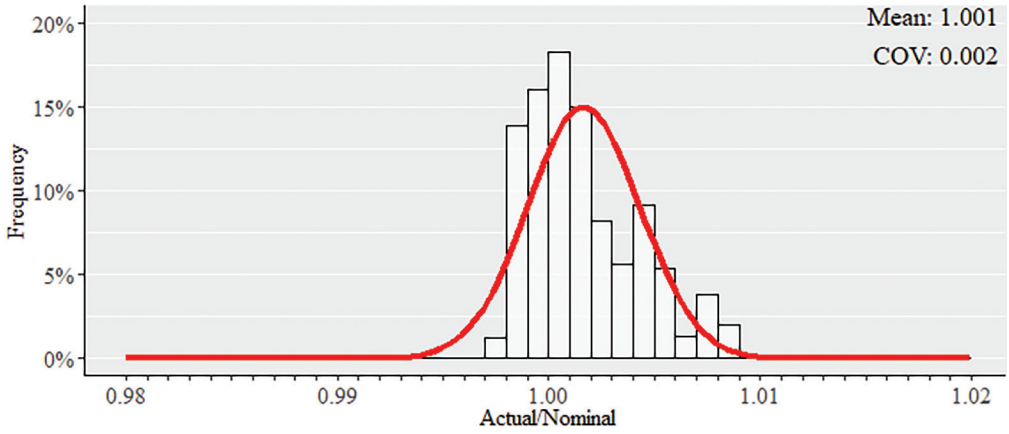

Fig. 7. Rectangular HSS depth and width variation data by Kennedy and Gad Aly (1980).

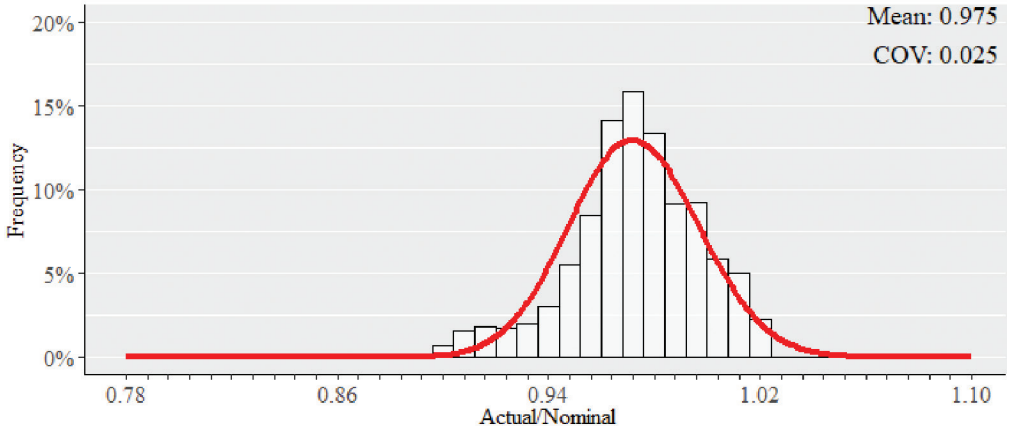

Fig. 8. Rectangular HSS thickness variation data by Kennedy and Gad Aly (1980).

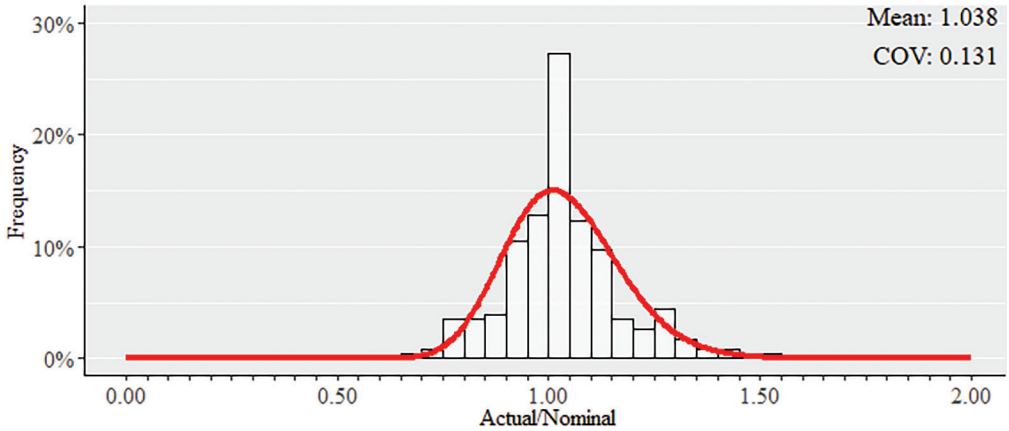

Fig. 9. Professional factors using the Wei and Packer (2021) proposed buckling method.

procedure was then repeated for a range of L/D ratios from 0 to 3.0; for resistance factors of 0.8, 0.85 and 0.90; and for each representative connection. For all simulations, the overall load effect distribution is approximately log-normal, and similarly, the resistance distribution is approximately log-normal, despite deviations from log-normality in the material survey and professional factor data, as shown previously. Thus, Equation 16, where the resistance and load effect distributions are both log-normal, can be used. Figures 10 and 11 display typical resistance and load effect distributions, respectively, determined for the set of representative connections.

MCS Results

A reliability index at each L/D ratio and resistance factor was determined by taking the average reliability index from each of the 19 connections. Figure 12 shows that $\phi = 0.90$ achieves suitable results as the reliability index is greater than 3.0 for the majority of the L/D ratios investigated and does not fall below 2.6 for any L/D ratio, which is the minimum that is currently expected (Commentary to 2016 AISC *Specification* Section B3.1).

The 19 representative connections cover the key variables in rectangular HSS-to-HSS cross connections. To investigate the chord sidewall slenderness effect, the average reliability index at each L/D ratio was determined for connections with the same chord sidewall slenderness (17.2, 22.9, 34.4, and 45.8, in the set of representative connections). Figure 13 shows that the reliability index decreases by about 0.1 when the chord sidewall slenderness is high (45.8). This is an expected result and is a reason the upper limits of validity have been set on chord sidewall slenderness in rectangular HSS cross connections. To investigate the bearing length effect, the average reliability index at each L/D ratio was determined for the connections in three categories: bearing length ratio ($H_b/H\sin\theta$) less than 1.0,

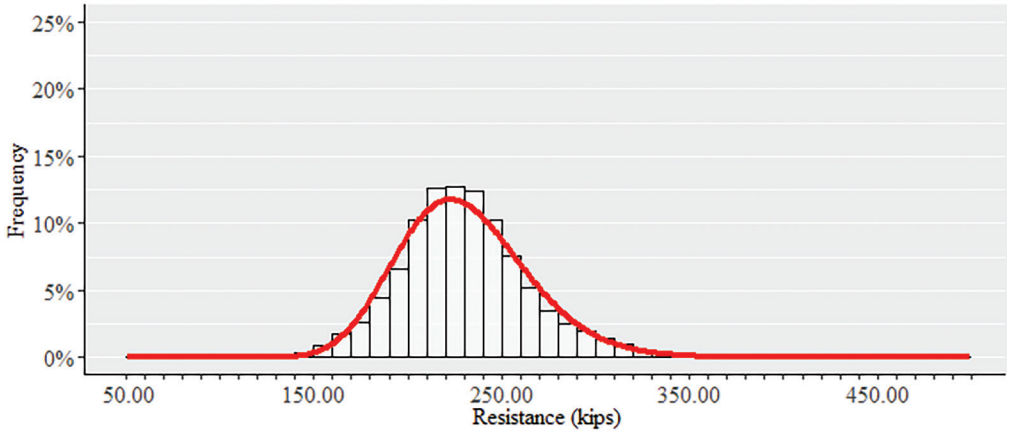

Fig. 10. Resistance for Connection 6, with L/D = *1.0 and* $\phi = 0.90$.

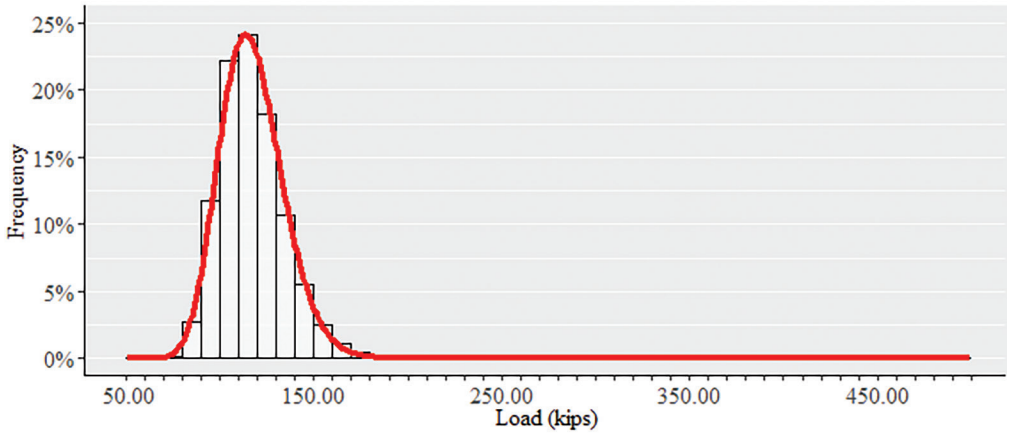

Fig. 11. Load effect for Connection 6, with L/D = *1.0 and* $\phi = 0.90$.

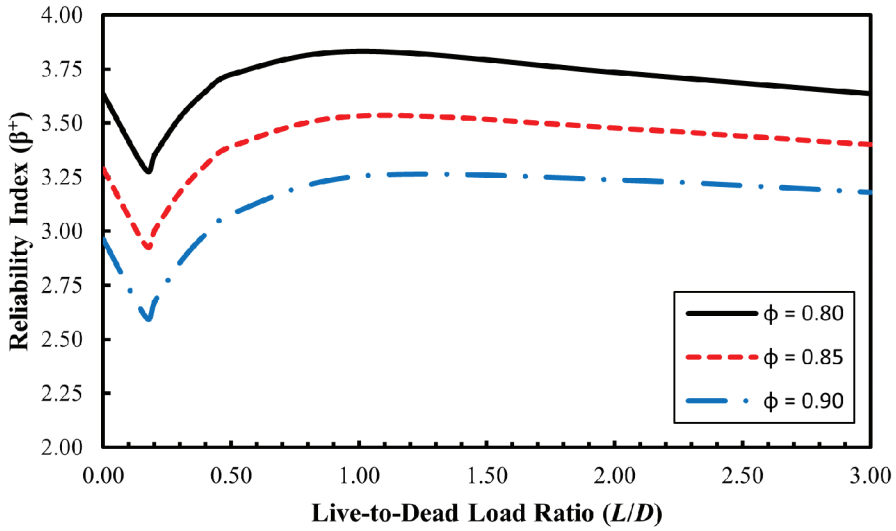

Fig. 12. Reliability index vs. L/D *ratio for the Wei and Packer (2021) proposed buckling method, using a MCS with various* ϕ *factors.*

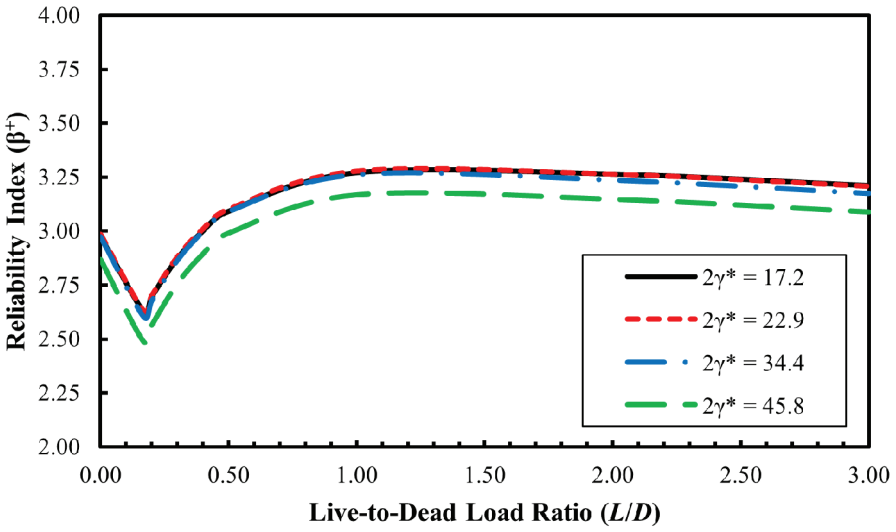

Fig. 13. Effect of chord sidewall slenderness on reliability index, for the Wei and Packer (2021) proposed buckling method, by MCS with ϕ *= 0.90.*

bearing length ratio between 1.0 and 2.0, and bearing length ratio greater than 2.0. Figure 14 illustrates that the bearing length effect is captured well by the proposed method.

SUMMARY

The closed-formed solution methods produce a resistance factor based on an input target reliability index, whereas the MCS method used herein produces a reliability index given a resistance factor. In order to compare the various reliability methods, the closed-formed solutions were manipulated to input a resistance factor and output a reliability index. The AISI S100-16 method is henceforth discounted due to its set target reliability of 2.5; the target reliability index for all other closed-form methods and the MCS method is 3.0. The separation factor approach and the expanded separation factor approach are independent of the L/D ratio; therefore, the reliability index for these methods applies to all L/D ratios. Figures 15 and 16 compare each of the methods, using $\phi = 0.90$.

The closed-form equations using the material statistical parameters adjusted for slenderness produce more conservative estimates of the reliability index compared to the yield stress material statistical parameters. This is expected as the mean-to-nominal ratio of the material statistical parameters adjusted for slenderness is lower.

MCS is a numerical method and is the most accurate reliability analysis. Using the yield stress parameters, the approximate FORM analysis in CSA S408-11 produces reliability index values that are within 0.10 of the MCS for all L/D ratios (Figure 15). Using the parameters adjusted for slenderness, the approximate FORM analysis in CSA S408-11 produces statistically indistinguishable reliability index values for $L/D \leq 0.50$, and values within 0.25 of the MCS (but on the conservative side) for $L/D > 0.50$ (Figure 16).

The expanded separation factor approach generates an unconservative reliability index value for $L/D \leq 0.50$, no matter which set of material statistical parameters are used. For $L/D > 0.50$, the yield stress parameters produce a surprisingly accurate reliability index value that is within 0.05 of the MCS values, while the parameters adjusted for slenderness produce a conservative reliability index value by about 0.30. The closed-form equations using the material statistical parameters of the yield stress create more accurate predictions of the reliability index (measured against MCS) than the case of material parameters adjusted for slenderness. All further comparisons are therefore based on the closed-form equations using yield stress material statistical parameters.

The separation factor approach produces extremely conservative predictions of the reliability index. This is expected since it only accounts for the professional factor.

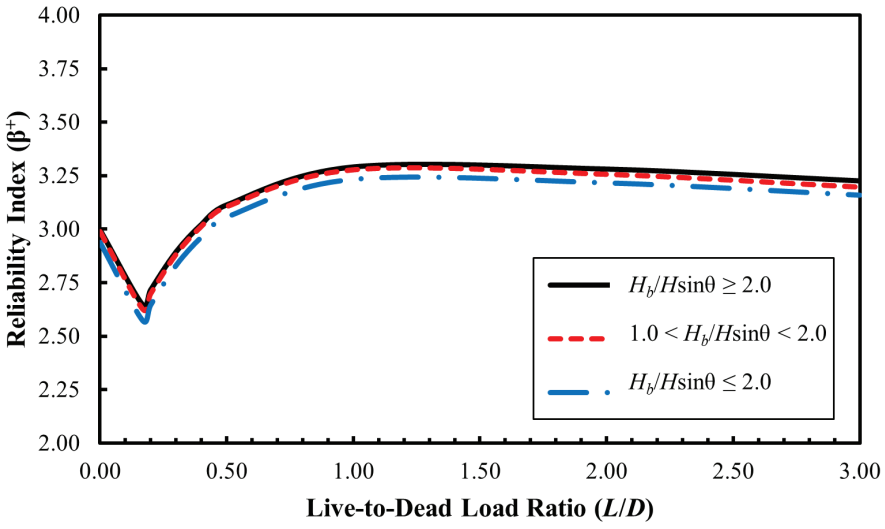

Fig. 14. Effect of bearing length on reliability index, for the Wei and Packer (2021) proposed buckling method, by MCS with $\phi = 0.90$.

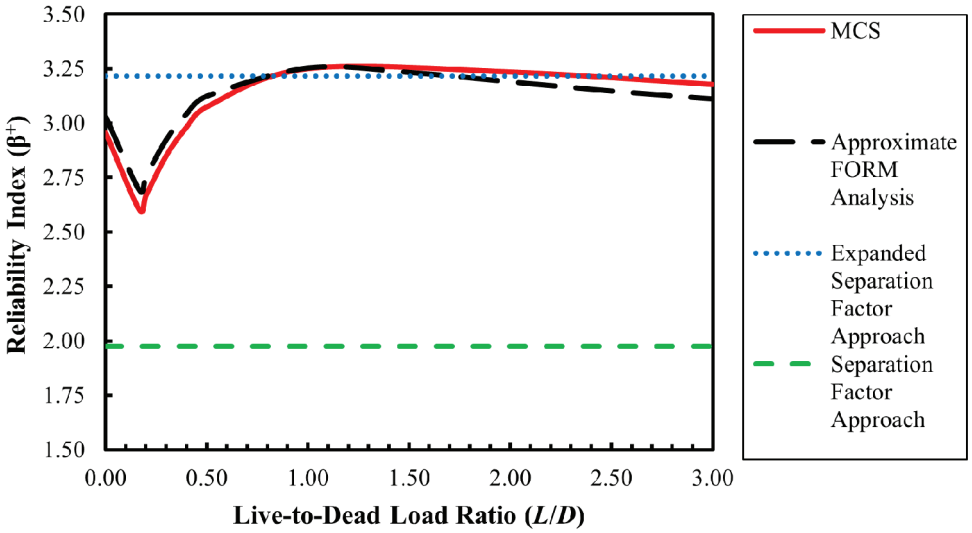

Fig. 15. Reliability index vs. L/D *ratio for the Wei and Packer (2021) proposed buckling method, using closed-form solutions and MCS, with yield stress material statistical parameters.*

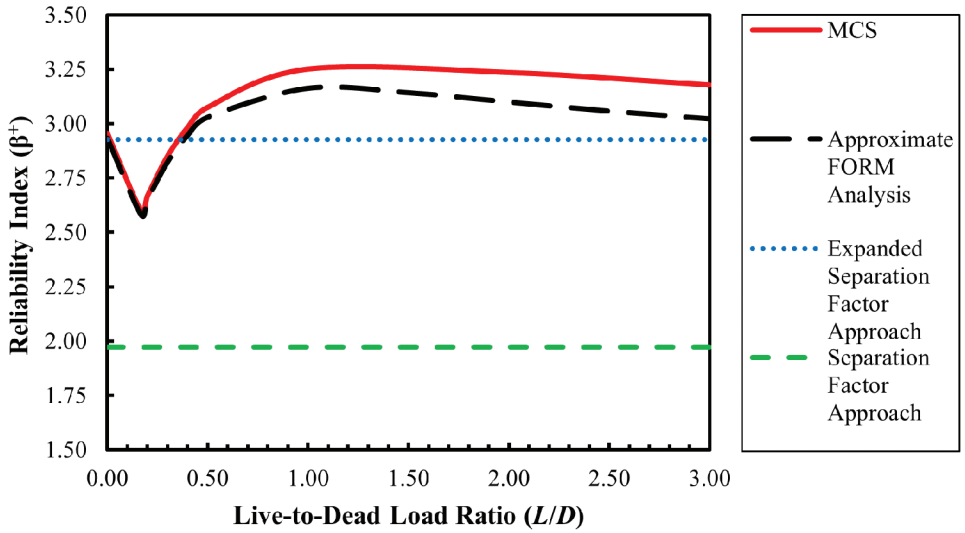

Fig. 16. Reliability index vs. L/D *ratio for the Wei and Packer (2021) proposed buckling method, using closed-form solutions and MCS, with material statistical parameters adjusted for chord slenderness.*

The expanded separation factor approach method produces much better predictions of the reliability index than the separation factor approach because it accounts for the material, geometric, and strength properties, as well as the professional factor. The material strength property (F_y) actual-to-nominal ratio usually has a mean (bias) much greater than 1.0 for HSS, and this is the main contributing factor in generating higher predictions for the reliability index. The expanded separation factor approach can still produce unconservative results for $L/D < 1.0$. For steel buildings, however, typical design L/D ratios exceed 1.0, and the expanded separation factor approach provides accurate predictions in this L/D range due to the uncertainties in live loading.

The approximate FORM analysis from CSA S408-11 thus appears ideal for determining the reliability index of HSS connections. This method illustrates the dependency of the reliability index on the L/D ratio and generates results that are very similar to MCS, yet requires much less time and effort to complete. From the preceding analysis, it can be concluded that, for the Wei and Packer (2021) proposed buckling method, $\phi = 0.90$ is appropriate. With this resistance factor, the reliability index is greater than 3.0 for the majority of the L/D ratios assessed and does not fall below 2.6 for any L/D ratio—the minimum currently expected (Commentary to the 2016 AISC *Specification* Section B3.1).

SIDEWALL LOCAL YIELDING

The approximate FORM analysis from CSA S408-11 was also used to evaluate Equation 1 (Table 1) for the sidewall local yielding limit state by using the existing database from Wei and Packer (2021). The resulting professional factor statistical parameters for Equation 1, in conjunction with this database, are $\delta_P = 1.193$ and $V_P = 0.150$ (Xi and Packer, 2021). Figure 17 shows the reliability index determined for the range of L/D ratios with $\phi = 1.0$. The reliability index is greater than 3.0 for most L/D ratios assessed and does not fall below 2.6 for any L/D ratio, thus supporting the choice of $\phi = 1.0$ for the Wei and Packer (2021) proposed local yielding design equation.

CONCLUSION

Several alternative methods for predicting the nominal strength of HSS webs under local compression loading are evaluated using a large contemporary database of experimental and numerical results totaling 227 tests. For rectangular HSS-to-HSS full-width cross connections under branch axial compression, it is found that the proposal of Wei and Packer (2021) accurately predicts the connection strength, without the further modifications suggested by Kim and Lee (2021). It is thus recommended that the Wei and Packer (2021) proposed approach for chord sidewall compression on rectangular HSS-to-HSS axially loaded cross connections (given in Table 1) be adopted. Monte Carlo simulation shows that the reliability index decreases for connections with a high chord sidewall slenderness; it is therefore recommended that the limit on chord sidewall slenderness be $H/t \leq 35$. Three key points for the Commentary to the AISC *Specification*, to facilitate the application of Chapter J to rectangular HSS sidewall compression, are:

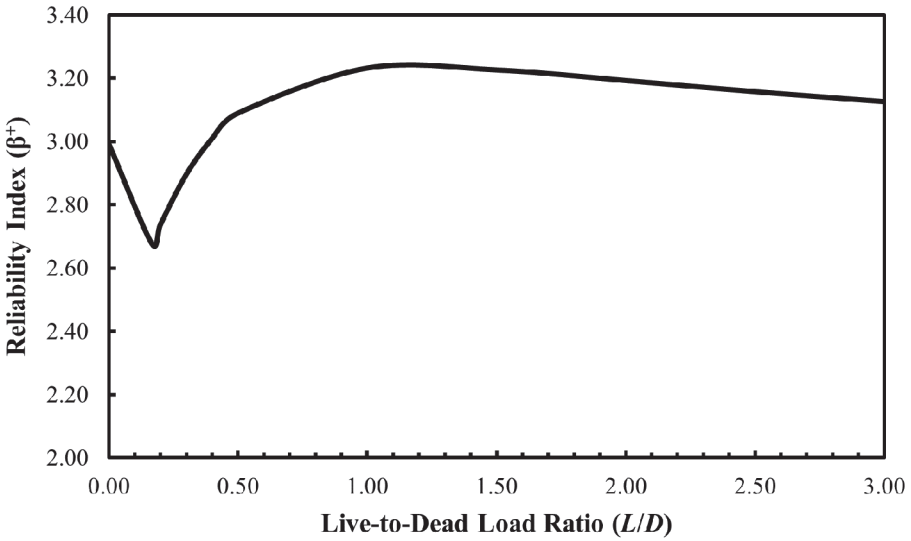

Fig. 17. Reliability index vs. L/D *ratio for Wei and Packer (2021) proposed local yielding equation, using the approximate FORM analysis in CSA S408-11.*

1. An effective length factor of $K = 0.65$ is recommended because it represents the fixed-fixed end condition for the chord sidewalls, in welded connections.
2. The F_{cr} equation (column buckling method) should be used for a bearing length greater than 0.25 of the chord depth.
3. The branch angle of inclination should not be considered because assuming only vertical force components is conservative, pragmatic, and simple.

A reliability analysis was performed for the Wei and Packer (2021) proposed web compression buckling method. This was assessed using various closed-form methods as well as a Monte Carlo simulation. Comparing all the reliability methods, an approximate FORM analysis given in CSA S408-11 produced excellent results, comparable to Monte Carlo simulation. The approximate FORM analysis generates a reliability index for any desired live-to-dead load ratio, avoids the complexity of Monte Carlo simulation, and is recommended. The review and application of contemporary reliability methods herein is instructive for other researchers determining resistance factors.

For the Wei and Packer (2021) proposed method for the web compression buckling limit state, a resistance factor of $\phi = 0.90$ is recommended, which is also the same value used for compression members in the AISC *Specification* Section E1. This resistance factor is included in Table 1 to determine available connection strength. The approximate FORM analysis in CSA S408-11 was also applied to evaluate the Wei and Packer (2021) proposed method for the web local yielding limit state, and a resistance factor of $\phi = 1.00$ is recommended. This is also the same value as used for this limit state in the AISC *Specification* Section J10.2, and this resistance factor is given for Equation 1 in Table 1.

ACKNOWLEDGMENTS

Financial support for this project was provided by MITACS and NSERC (Natural Sciences and Engineering Research Council of Canada). Appreciation is extended to Professor Judy Liu (Oregon State University) for provision of data.

SYMBOLS

A_g Cross-sectional area of element, in.^{2}

B Width of rectangular HSS chord member, perpendicular to the plane of the connection, in.

B_b Width of rectangular HSS branch member, perpendicular to the plane of the connection, in.

C_f Material factor

C_p Correction factor for sample size

C_ϕ Calibration coefficient

D Dead load, kips

E Modulus of elasticity of HSS member, ksi

F_{cr} Critical buckling stress of HSS chord member, ksi

F_k Chord sidewall failure stress, including a reduction for application to design, ksi

F_y Yield stress of HSS chord member, ksi

G Ratio of actual-to-nominal geometric property

H Height of rectangular HSS chord member, parallel to the plane of the connection, in.

H_b Height of rectangular HSS branch member, parallel to the plane of the connection, in.

K Effective length factor

L Live load, kips; length of member, in.

L_c Effective length of the member = KL, in.

M Ratio of actual-to-nominal material property

N_{1u} Axial ultimate strength of a connection for a test (or numerical calculation), expressed as a force in the branch, kips

N_{AISC} Axial ultimate strength of a connection, per the AISC *Specification*, expressed as a force in the branch, kips

N_{KL} Axial ultimate strength of a connection, per Kim and Lee (2021), expressed as a force in the branch, kips

N_L Axial ultimate strength of a connection, per Lan et al. (2021), expressed as a force in the branch, kips

N_{WP} Axial ultimate strength of a connection, per Wei and Packer (2021), expressed as a force in the branch, kips

P Professional factor = ratio of observed capacity in tests (experimental or numerical) to predicted capacity

P_n Connection nominal strength, kips

Q_f Chord-stress interaction parameter

R Resistance, kips

R_m Mean resistance, kips

R_n Nominal resistance, kips

R_t Tested resistance/strength, kips

S Load effect, kips

S_m Mean load effect, kips

S_n Nominal load effect, kips

V_D Coefficient of variation for dead load

V_E Coefficient of variation for modulus of elasticity

V_G Coefficient of variation for relevant geometric properties

V_L Coefficient of variation for live load

V_M Coefficient of variation for relevant material properties

V_P Coefficient of variation associated with δ_P

V_R Coefficient of variation for resistance

V_r Coefficient of variation for radius of gyration

V_S Coefficient of variation for load effect

g Safety margin

g_m Mean of the safety margin

i Subscript that denotes the load effect under consideration (dead, live, etc.); subscript that denotes an individual test

l_b Bearing length of the load, measured parallel to the axis of the chord member, in.

l_{end} Distance from the near side of the connecting branch or plate to the end of chord, in.

m Degrees of freedom, $n_t - 1$

n_0 Ratio of stress in the chord connecting face to the chord yield stress (+ indicates chord tensile stress; − indicates chord compressive stress)

n_t Number of tests

p_F Probability of failure

r Radius of gyration, in.

t Design wall thickness of rectangular HSS chord member, in.

t_b Design wall thickness of rectangular HSS branch member, in.

Ω Safety factor

α Coefficient of separation, generally taken as 0.55

α_D Load factor for dead load

α_L Load factor for live load

β Ratio of branch width to chord width (B_b/B), perpendicular to the plane of the connection

β^+ Reliability or safety index

2γ Ratio of chord width to wall thickness for rectangular HSS (B/t)

$2\gamma^*$ Ratio of chord height to wall thickness for rectangular HSS (H/t)

δ_D Ratio of mean to nominal for dead load

δ_E Ratio of mean to nominal for modulus of elasticity

δ_G Mean value of G

δ_L Ratio of mean to nominal for live load

δ_M Mean value of M

δ_P Mean value of P

δ_R Ratio of mean to nominal for resistance

δ_r Ratio of mean to nominal for radius of gyration

δ_S Ratio of mean to nominal for load effect

η Ratio of branch height to chord width for rectangular HSS (H_b/B)

η^* Ratio of branch height to chord height for rectangular HSS (H_b/H)

θ Acute angle between the branch and chord, degrees

θ_C Central safety factor

λ Slenderness of a column or chord sidewall = KL/r

$\lambda_{0.65}$ Nondimensional chord sidewall slenderness with an effective length factor of 0.65

$\lambda_{1.0}$ Nondimensional chord sidewall slenderness with an effective length factor of 1.0

λ_C Nondimensional chord sidewall slenderness

λ_{KL} Nondimensional chord sidewall slenderness with the Kim and Lee (2021) effective length factor

σ_P Standard deviation of the ratio of actual-to-nominal strength

σ_R Standard deviation of R

σ_S Standard deviation of S

σ_g Standard deviation of g

ϕ Resistance factor

χ Reduction factor for (column) buckling

REFERENCES

AISC (2016), *Specification for Structural Steel Buildings*, ANSI/AISC 360-16, American Institute of Steel Construction, Chicago, Ill.

AISI (2016), *North American Specification for the Design of Cold-Formed Steel Structural Members*, AISI S100-16, American Iron and Steel Institute, Washington, D.C.

ASCE (2016), *Minimum Design Loads and Associated Criteria for Buildings and Other Structures*, ASCE/SEI 7-16, American Society of Civil Engineers, Reston, Va.

ASTM (2021), *Standard Specification for Cold-Formed Welded and Seamless Carbon Steel Structural Tubing in Rounds and Shapes*, ASTM A500/A500M-21, ASTM International, West Conshohocken, Pa.

Benjamin, J.R. and Cornell, C.A. (1970), *Probability, Statistics, and Decision for Civil Engineers*, McGraw-Hill, New York, N.Y.

Bu, X.D., Wei, F., and Packer, J.A. (2021), "Laterally Offset RHS X-Connections," *Journal of Structural Engineering*, ASCE, Vol. 147, No. 1, 04020286.

CEN (2021), *Eurocode 3: Design of Steel Structures—Part 1–8: Design of Joints*, prEN 1993-1-8, European Committee for Standardization, Brussels, Belgium.

CSA (2011), *Guidelines for the Development of Limit States Design Standards*, CSA S408-11, Canadian Standards Association, Toronto, Canada.

CSA (2019a), *Design of Steel Structures*, CSA S16:19, Canadian Standards Association, Toronto, Canada.

CSA (2019b), *Canadian Highway Bridge Design Code*, CSA S6:19, Canadian Standards Association, Toronto, Canada.

Davies G. and Roodbaraky K. (1987), "The Effect of Angle on the Strength of RHS Joints," *Proceedings of the International Meeting on Safety Criteria in Design of Tubular Structures*, Tokyo, Japan.

Ellingwood, B. and Culver, C. (1977), "Analysis of Live Loads in Office Buildings," *Journal of the Structural Division*, ASCE, Vol. 103, No. 8, pp. 1,551–1,560.

Ellingwood, B., Galambos, T.V., MacGregor, J.G., and Cornell, C.A. (1980), "Development of a Probability Based Load Criterion for American National Standard A58," *Special Publication 577*, National Bureau of Standards, Gaithersburg, Md.

Fan, Y. (2017), "RHS-to-RHS Axially Loaded X-Connections Offset towards an Open Chord End," M.A.Sc. Thesis, University of Toronto, Toronto, Canada.

Feldmann, M., Schillo, N., Schaffrath, S., Virdi, K., Björk, T., Tuominen, N., Veljkovic, M., Pavlovic, M., Manoleas, P., Heinisuo, M., Mela, K., Ongelin, P., Valkonen, I., Minkkinen, J., Erkkilä, J., Pétursson, E., Clarin, M., Seyr, A., Horváth, L., Kövesdi, B., Turán, P., and Somodi, B. (2016), "Rules on High Strength Steel," Publications Office of the European Union, Luxembourg.

Galambos, T.V. (2006), "Reliability of the Member Stability Criteria in the 2005 AISC Specification," *International Journal of Steel Structures*, Vol. 4, No. 4, pp. 223–230; and *Engineering Journal*, AISC, Vol. 43, No. 4, pp. 257–265.

Galambos, T.V. and Ravindra, M.K. (1973), "Tentative Load and Resistance Factor Design Criteria for Steel Buildings," Research Report No. 18, Civil and Environmental Engineering Department, Washington University, St. Louis, Mo.

Galambos, T.V. and Ravindra, M.K. (1977), "The Basis for Load and Resistance Factor Design Criteria of Steel Building Structures," *Canadian Journal of Civil Engineering*, Vol. 4, pp. 178–189.

Galambos, T.V. and Ravindra, M.K. (1978), "Properties of Steel for Use in LRFD," *Journal of the Structural Division*, ASCE, Vol. 104, No. 9, pp. 1,459–1,468.

Hong, H.P. and Zhou, W. (1999), "Reliability Evaluation of RC Columns," *Journal of Structural Engineering*, ASCE, Vol. 125, No. 12, pp. 784–790.

IIW (2012), *Static Design Procedure for Welded Hollow Section Joints—Recommendations*, 3rd Ed., IIW Doc. XV-1402-12, International Institute of Welding, Genoa, Italy.

ISO (2013), *Static Design Procedure for Welded Hollow Section Joints—Recommendations*, ISO 14346, International Organization for Standardization, Geneva, Switzerland.

Kennedy, D.J.L. and Baker, K.A. (1984), "Resistance Factors for Steel Highway Bridges," *Canadian Journal of Civil Engineering*, Vol. 11, pp. 324–334.

Kennedy, D.J.L. and Gad Aly, M. (1980), "Limit States Design of Steel Structures—Performance Factors," *Canadian Journal of Civil Engineering*, Vol. 7, pp. 45–77.

Kim, J.H., Lee, C.H., Kim, S.H., and Han, K.H. (2019), "Experimental and Analytical Study of High-Strength Steel RHS X-Joints under Axial Compression," *Journal of Structural Engineering*, ASCE, Vol. 145, No. 12, 04019148.

Kim, S.H. and Lee, C.H. (2021), "Chord Sidewall Failure of RHS X-Joints in Compression and Associated Design Recommendations," *Journal of Structural Engineering*, ASCE, Vol. 147, No. 8, 04021111.

Kuhn, J. (2018), "Numerical Study of Full-Width, RHS-to-RHS, X-Connections under Transverse Compression," Master's Thesis, Karlsruhe Institute of Technology, Karlsruhe, Germany.

Kuhn, J., Packer, J.A., and Fan, Y. (2019), "Rectangular Hollow Section Webs under Transverse Compression," *Canadian Journal of Civil Engineering*, Vol. 46, pp. 810–827.

Lan, X., Wardenier, J., and Packer, J.A. (2021), "Design of Chord Sidewall Failure in RHS Joints Using Steel Grades up to S960," *Thin-Walled Structures*, Vol. 163, 107605.

Lind, N.C. (1971), "Consistent Partial Safety Factors," *Journal of the Structural Division*, ASCE, Vol. 97, No. 6, pp. 1,651–1,670.

Liu, J. (2016), "Updates to Expected Yield Stress and Tensile Strength Ratios for Determination of Expected Member Capacity in the 2016 AISC Seismic Provisions," *Engineering Journal*, AISC, Vol. 53, No. 4, pp. 215–228.

Lundberg, J.E. and Galambos, T.V. (1996), "Load and Resistance Factor Design of Composite Columns," *Structural Safety*, Vol. 18, pp. 169–177.

Meimand, V.Z. and Schafer, B.W. (2014), "Impact of Load Combinations on Structural Reliability Determined from Testing Cold-Formed Steel Components," *Structural Safety*, Vol. 48, pp. 25–32.

Melchers, R.E. and Beck, A.T. (2018), *Structural Reliability Analysis and Prediction*, 3rd Ed., Wiley, Hoboken, N.J.

NBC (2020), *National Building Code of Canada*, NBC 2020 Part 4, National Research Council, Ottawa, Canada.

Nowak, A.S. and Lind, N.C. (1979), "Practical Bridge Code Calibration," *Journal of the Structural Division*, ASCE, Vol. 105, No. 12, pp. 2,497–2,510.

Packer, J.A. and Kremer, J.S.M. (1988), "A Reliability Assessment of Tubular Joint Specifications," *Canadian Journal of Civil Engineering*, Vol. 15, pp. 167–175.

Packer, J.A., Wardenier, J., Zhao, X.L., van der Vegte, G.J., and Kurobane, Y. (2009), *Design Guide for Rectangular Hollow Section (RHS) Joints under Predominantly Static Loading*, CIDECT Design Guide No. 3, 2nd Ed., CIDECT, Geneva, Switzerland.

Pandey, M. and Young, B. (2020), "Structural Performance of Cold-Formed High Strength Steel Tubular X-Joints under Brace Axial Compression," *Engineering Structures*, Vol. 208, 109768.

Ravindra, M.K. and Galambos, T.V. (1978), "Load and Resistance Factor Design for Steel," *Journal of the Structural Division*, ASCE, Vol. 104, No. 9, pp. 1,337–1,353.

Rudman, D.F. (2021), "Reliability of RHS X-Connections in Branch Axial Compression," M.A.Sc. Thesis, University of Toronto, Toronto, Canada.

Schmidt, B.J. and Bartlett, F.M. (2002), "Review of Resistance Factor for Steel: Resistance Distributions and Resistance Factor Calibration," *Canadian Journal of Civil Engineering*, Vol. 29, pp. 109–118.

Wardenier, J., Lan X.Y., and Packer J.A. (2020), "Evaluation of Design Methods for Chord Sidewall Failure in RHS Joints Using Steel Grades up to S960—State of the Art," IIW Doc. XV-E-489-20.

Wei, F. and Packer, J.A. (2021), "AISC Provisions for Web Stability under Local Compression Applied to HSS," *Engineering Journal*, AISC, Vol. 58, No. 1, pp. 11–32.

Xi, Q. and Packer, J.A. (2021), "Assessing the Probabilistic Assumptions behind Structural Reliability via Simulation," Canadian Society for Civil Engineering Annual Conference, Virtual, Canada, STR230.

Yu, Y. (1997), "The Static Strength of Uniplanar and Multiplanar Connections in Rectangular Hollow Sections," Ph.D. Thesis, Delft University of Technology, Delft, The Netherlands.